AN UPDATE ON MODELLING THE OHAAKI GEOTHERMAL SYSTEM

E.K. Clearwater[1], M.J. O'Sullivan[1], and K. Brockbank[2]

[1]Department of Engineering Science, University of Auckland, Private Bag 92019, Auckland 1142, New Zealand

[2]Wairakei Power Station, Contact Energy, State Highway 1, Private Bag 2001, Taupo 3352, New Zealand

ecle011@aucklanduni.ac.nz

Keywords: *Ohaaki, Geothermal, Modelling, TOUGH2, Leapfrog Geothermal.*

ABSTRACT

Since the Ohaaki power station was commissioned in 1988, a series of large three-dimensional numerical models of the Ohaaki geothermal system have been developed at the University of Auckland in collaboration with Contact Energy and its predecessors. Over the course of 2010 and 2011 the model has been reviewed and re-calibrated in order to improve the match between measured data and model results. This was part of an ongoing effort to represent the Ohaaki system more accurately, so that the model can be used to better predict the future behaviour of the resource.

Updates of the model grid include horizontal and vertical refinement. During the calibration process some adjustments were made to the deep upflow of very hot water and CO_2 at the base of the model. Also some adjustments were made to permeabilities and porosities, including the use of the LEAPFROG software to make the rock type assignment in our reservoir model better match the geological model developed by Contact Energy and GNS Science.

Natural state simulations were used to compare the model results to the temperature data for the pre-exploitation state of the reservoir. Then production history simulations were carried out and pressure, temperature, CO_2 flow and enthalpy data were compared to model results, using data from the well testing period, the recovery period and the production period. Overall, a significant improvement in the model match has been made compared to the previous (2006) model.

1. INTRODUCTION

The Ohaaki geothermal system lies on the eastern margin of the Taupo Volcanic Zone. The Waikato River bisects the Ohaaki system, dividing it into the West Bank and East Bank areas (Figure 1). Drilling commenced at Ohaaki in 1965, with a total of 44 wells drilled between 1966 and 1984. There was an extended period of well testing and recovery up to 1988, when the Ohaaki Geothermal Power station was commissioned [1]. There are now over 65 wells drilled in the area.

A sequence of numerical models of the Ohaaki System have been set up by O'Sullivan and co-workers (e.g. [2],[3]). As computer hardware and software improved these models increased in complexity and evolved into the large three-dimensional models described here.

Two computer models of the Ohaaki geothermal system are discussed in the present paper, both resulting from a recent review and re-calibration of the computer model as it existed in 2006 and as described by Zarrouk and O'Sullivan [4]. The aim in developing these models was to improve the match between model results and measured data and in turn to try to represent the Ohaaki system more accurately. This was done by changing the heat, mass and CO_2 input at the base of the model and by adjusting the permeability structure.

The first model to be discussed, called here the 2010 model, was reported by O'Sullivan and Clearwater [5]. The 2010 model was then modified to create the current Ohaaki model - the 2011 model. For this model the vertical layer structure was refined, and the geological model was more accurately represented.

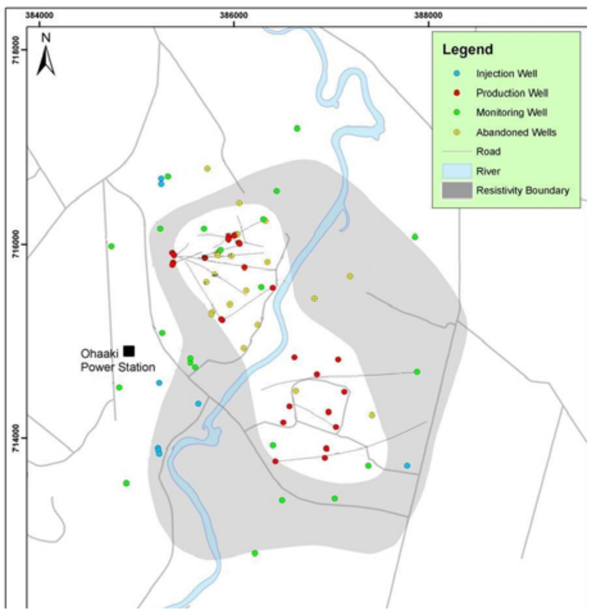

Figure 1: The Ohaaki Field.

2. OHAAKI GEOTHERMAL SYSTEM

Ohaaki is a high temperature convective system. The two phase reservoir has a base temperature in excess of 300°C and has substantial quantities of non condensable gases, primarily CO_2. The large amount of CO_2 makes the field response very different to that for a conventional hot water system (e.g.Wairakei).

The natural heat flow is thought to be approximately 100MW [6], but discharge into the Waikato River was not well quantified prior to production and so this figure may not be accurate. There was little geothermal activity seen on the surface, but what did exist covered a total area of 10km² over the whole field and was concentrated into two zones, the most pronounced being on the West Bank with a line of steam heated ground and pools [7]. The most dominant feature was the Ohaaki Pool, which discharged boiling neutral chloride water at about 9l/s and had extensive sinter deposits around the edges of the pool [8].

The basement of the system is a pre-volcanic greywacke which down faults to the north-west. There is little matrix permeability and porosity, and the fractures have not shown much permeability either [9]. Overlying this is a volcano-clastic sequence interspersed with dacitic and rhyolitic volcanic domes and flows.

The first formation overlying the basement is the Tahorakuri Formation. This contains the Waikora formation – a pebbly greywacke derived conglomerate - along with andesite and dacite bodies. Overlying this is the Rangitaiki Ignimbrite which has very low permeability. Above the ignimbrite lies the Rautawiri Breccia which appears to be permeable at its contacts with the under and overlying formations. Above the breccia is a low permeability siltstone along with various volcanic flows such as the Broadlands Dacite. Overlying this is the Waiora formation which has good permeability, but there is no obvious pattern to the permeability distribution. Above the Wairoa lies the Huka Falls Formation which generally acts as an impermeable cap to the system, but has areas of local permeability. Interspersed within the Huka Falls are the Ohaaki and Broadlands Rhyolites, These shallow rhyolites tend to be permeable to shallow steam-heated fluids. [10],[11]

The plant commissioned in 1988 was 116MW$_e$ and during the first 5 years of production, generation was maintained at ~100MW$_e$. In 1993 the available steam began to decline, power generation decreased and discharge from the Ohaaki pool ceased. These early production zones were concentrated within the volcano-clastic cover (generally within the Waiora formation below the rhyolites). The extraction of production fluid caused a significant pressure drawdown and a reduction in the water level - monitoring wells showed the water level decreased by up to 10m. Steam flow to the surface declined and cool fluids entered parts of the reservoir. This was partly due to returns of reinjected water and partly due to cold downflows through the Ohaaki Rhyolite. These effects reduced the steam zone and caused the production wells to cool [12].

In 1995, to try and counteract this steam decline, a deep drilling program was undertaken which identified high temperatures and permeability in the deep volcanic formations underlying the West Bank [10],[1]. This was relatively successful, however even with these new productive wells and regular workovers to prevent calcite scaling, steam supply continued to decline, albeit at a reduced rate. Generation dropped down to 25-40MW$_e$. A second deep drilling program also focused on the West Bank was undertaken in 2005-2007, the success of this allowed generation output to be maintained above 60MW$_e$. At the end of 2009 the output was starting to decline again.

3. FIELD DATA

In order to calibrate the natural state simulation, temperature data is required. There are measurements available of downhole temperatures for most of the Ohaaki wells, as well as interpretations of these to provide the best estimates of natural state reservoir temperatures.

To model the well testing period and production history, injection and production data are required. Unfortunately, a continuous record of production data from individual wells at Ohaaki is not available. This is due to the limitations of accurately measuring two-phase flow at the time of commissioning the power plant. Instead the combined mass flow and total production enthalpy data from each separator is provided.

There are five separators at Ohaaki – one of which has been decommissioned since 2007. The existing four separators have between three and eight wells connected to them, and the total mass and enthalpy data regularly recorded is the combined flow for that specific group of wells.

For each well the operating well head pressure is also recorded regularly, along with the status of the well (whether it is on production, on bleed, closed, reinjecting, etc). The number of days per week that the well is on production is recorded, and thus the proportion of each week that each well is open is available. Individual wells are output tested every six months, and these tests provide characteristic curves for each well from which it is possible to derive a flowrate given the measured wellhead pressure. From the calculated flow rate and the open times for each well, a weekly mass flow can be calculated, by multiplying the mass flow per week by the proportion of open time.

Data from the performance of the wells during the occasional output tests are used to calculate the proportion from each well supplying a particular separator. Finally, these proportions are used to calculate weekly flows for each well to be used in the model. The measured average weekly separator flow is multiplied by the proportion of flow calculated for each well.

For multi-feed wells the production is further broken down by assigning a proportion of the total flow rate to each feed.

Neither of these procedures, first of using the occasional output test data to assign separator flows to individual wells in order to obtain continuous records of well by well production and secondly of assigning set proportions to multi-feed wells, is entirely satisfactory. The well characteristic curves and proportion of the contribution from each well to the separator vary from one output test to the next and the enthalpy response of the model is quite sensitive to flowrate. So this approach to creating production rates may lead to incorrect model enthalpies.

Entering the injection data into the model is much simpler and more accurate – continuous injection rates for each injection well are provided.

For calibration of the well testing period and production history, pressure, enthalpy and CO_2 fraction data are required. Continual pressure data is available from monitoring wells throughout the field. The well output tests provide pressure, production enthalpy and CO_2 flow as a percentage of total flowrate for individual wells.

4. 2010 RESERVOIR MODEL

The 2010 model is a development of the 2006 model, reported in [4], which in turn is based on the previous 2004 model, reported in [13]. The grid for the 2006 model contained 393 grid blocks per layer and covers the same area as the 2004 model (18km by 18km). The 2010 grid has 992 blocks per layer and covers a slightly smaller horizontal area (16km by 15km). These two grids are shown in Figure 2 for comparison. Note that because the area depicted is the same for each image in Figure 2, the corner blocks of the 2006 grid have been cropped, an indication of the larger area covered by this grid.

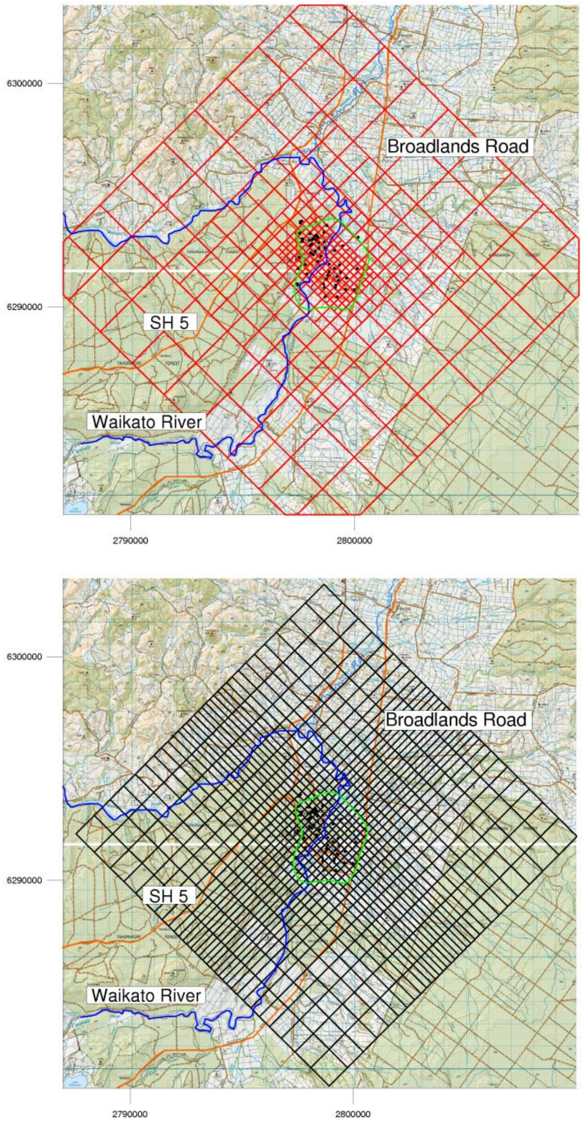

Figure 2. The 2006 grid (top image, red grid) and the 2010 model grid (bottom image, black grid). The Waikato River is shown in blue, the resistivity boundary in green and wells in black.

Figure 3 shows that the 2006 grid structure had five noded blocks with some large blocks joined to two smaller ones. This is computationally undesirable, although the grid allowed most wells to be allocated to separate blocks. The 2010 grid has a gradual expansion of block size, instead of using locally refined areas. The smallest blocks are 250m by 250m, and as the grid moves out from the central borefield area, the grid blocks expand to 1km by 1km. The block structure allows most wells to be placed in separate blocks; which is an improvement on the 2006 model for wells in reinjection areas and other marginal blocks.

The vertical layer structure of the 2006 model grid is the same as the 2004 model and was retained for the 2010 model. It includes a gradual transition to the thin layer representing the contact zone at the base of the rhyolite.

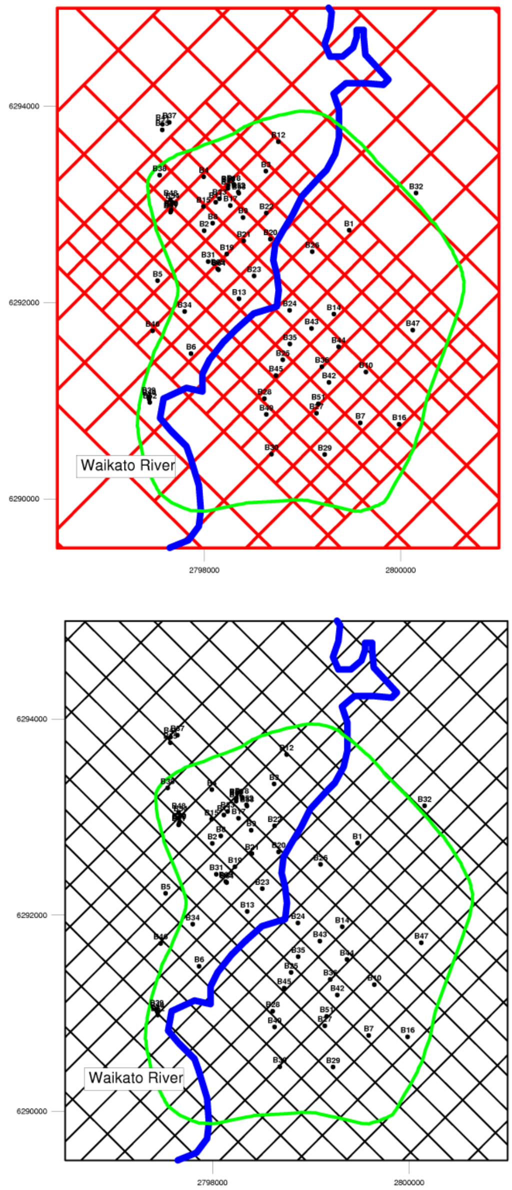

Figure 3. A close up of 2006 grid (top image, red) compared to the 2010 model grid (bottom image, black)

Adjustments to the heat, mass and CO_2 injected into the base of the model as boundary conditions, as well as permeability were made in order to gain a better match than the 2006 model to field data for both the natural state simulation and production history match. Results and further detail of the calibration are reported in [5].

5. 2011 RESERVOIR MODEL

5.1 Grid Structure

The 2011 model is a development of the 2010 model. The horizontal grid layout is the same as for the 2010 model and the only change to the grid structure is in the vertical layering. The gradual transition to the thin layer representing the contact zone at the base of the rhyolite is still included (-200mRL, layer 7), but the deepest five layers have been split in half to create 23 layers compared to 18 layers in the 2010 model (see Figure 4). This still gives the same total depth of the model, but allows for more vertical resolution for calibration of wells with deep feed zones, and more layers between the boundary blocks and bottom of the deepest wells.

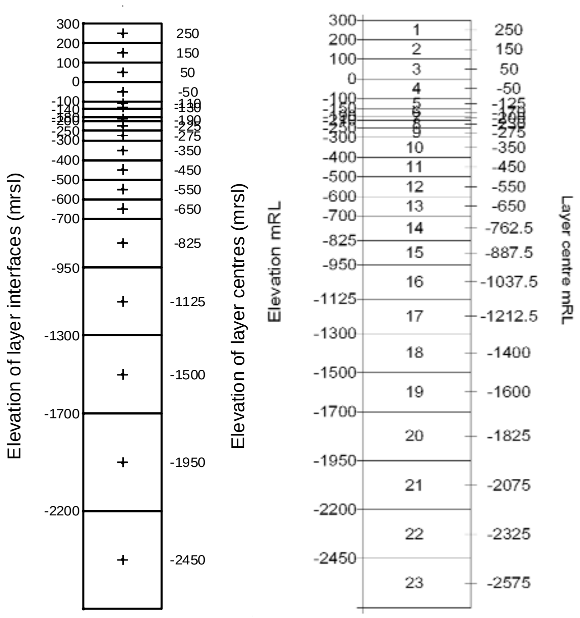

Figure 4. The 2006/2010 vertical layer structure of the model grid (left) compared to the 2011 grid layering (right).

5.2 Boundary Conditions

The boundary conditions applied to the 2011 model are the same as for the 2010 model and preceding models; although for the bottom boundary the flux values are varied as calibration proceeds.

The top of the model is located at the water table - this groundwater surface is assumed not to change very significantly during production. The groundwater surface calculated for the 2010 model was reapplied to the 2011 model, as the horizontal layer area and structure of the grid are unchanged. The top surface is open, and so water can flow in or out of the model. The temperature and pressure of the surface blocks are fixed at atmospheric conditions (pressure 1bar, temperature 15°C). This is only an approximation as the water table may be deep in some areas and the temperature may be above 15 degrees, however there is only a sparse set of shallow bore temperature data covering the region of the computational model, and so an approximation is necessary. An air/CO_2/water model with the top of the model at ground surface would remove this water table approximation, but currently there is no equation of state module within AUTOUGH2 that can handle the properties of air, water and CO_2 together in the unsaturated zone, and so the assumption is still required. Alternatively an artificial CO2 atmosphere could be used.

All four vertical sides of the model are treated as no-flow boundaries. This is a reasonable approximation for Ohaaki because of the high carbon dioxide content and the large boiling zone. Pressure changes in the reservoir are buffered by the expansion and contraction of the boiling zone and so do not spread to the edge of the model. Thus the horizontal grid area is deemed large enough to capture all the important behaviour of the Ohaaki system within it. There are no recharge boundary conditions on these sides of the model, and no set hydrostatic pressure and conductive temperature profiles.

At the base of the model a background conductive flow of heat is applied. For areas well outside the reservoir, a value of 120mW/m² is used, corresponding to the general background heat flux found in the Taupo Volcanic Zone. The heat flux is gradually increased for blocks nearer to the main reservoir, to represent the greater heat flow anomaly associated with the Ohaaki system, with a maximum heat flux value of 420mW/m². The value of heat flux in each block is adjusted as part of the calibration process.

Within the reservoir area, there is no conductive heat flow, and instead an upflow of hot water and carbon dioxide are included. The "reservoir area" is deemed to be blocks within and near the outer resistivity boundary, as defined by DC resistivity surveys [14, 15]. Mass flows are injected into these blocks with levels that increase according to the proximity to the main west and east bank reservoirs. The inner resistivity boundary is defined by the 270°C temperature contour measured at -600mRL, which is the limit of the productive reservoir. The blocks within this area have CO_2 as well as mass injected. The enthalpy and amount of mass or carbon dioxide content of the deep inflow are all adjusted as part of the calibration process. A summary of the total mass, heat and CO_2 injected into the model is shown in Table 1.

	Enthalpy (kJ/kg)	**Temperature (°C)**	**Total**
Mass (kg/s)	1428	314.4	68.32
Heat (MW)	-	-	39.64
CO_2 (kg/s)	1405	310.51	1.7

Table 1. Total flow into the base of the model.

The amount of carbon dioxide injected gives an average flowing mass fraction of 2.5%. By multiplying the amount of mass and CO_2 injected into each block by the respective enthalpy input and adding on the conductive heat flow we get a total heat input of 119.20MW. This value is very close to what the natural heat flow is thought to be, around 100MW. Due to the uncertainty of the quantification of the natural state value the model value of 119MW is thought to be reasonable.

5.3 Geoscience Data

Every block in the model grid is populated with a rock-type that has a certain permeability, porosity, density etc associated with it. To help decide on what parameters to set for different blocks, geoscience data is invaluable. Various geological models have been created over the years for Ohaaki, but until the recent University of Auckland collaboration with Leapfrog Geothermal [16] there has been no automated way to easily and quickly populate any TOUGH2 grid with a geological model. There has also never been any relation between the software used by modellers to update their models and manipulate the TOUGH2 input files, and the software used by geoscientists.

This new three-dimensional geological mapping software package allows reservoir modellers to view a compilation of different geological, geophysical and geochemical data and relate it to the reservoir model. There is a new integration between the geological model and the TOUGH2 grid; geological lithologies can be exported on to TOUGH2 grids.

The TOUGH2 grid itself can be loaded and any rock parameter visualized – allowing comparison with the geoscience data.

At the moment this tool provides a new three dimensional visualization interface and allows a fast set up of model grid rock-types. In the future it is hoped that Leapfrog Geothermal will also allow quicker and easier updates for model input data, initial model grid set up, and visualization of results.

5.4 Simulator

To solve the equations of flow of heat and mass through the numerical model created for Ohaaki, the geothermal simulator AUTOUGH2 [17] is used. This software is a modified version of TOUGH2 [18] developed at Auckland University. Due to the substantial amount of CO_2 present in the field, the EOS module used is that of water (two-phase) and CO_2, allowing us to keep track of and calibrate against the amount of CO_2 moving around the reservoir. The primary variables solved for at each time step are pressure, saturation (or temperature if single phase) and partial pressure of CO_2.

5.5 Natural State Modelling

In order to use the Ohaaki model for simulation of the effects of production, the model needs initial conditions. These initial conditions are a representation of the natural state of the field before the start of any production or well testing, a representation of its unchanging or natural state. For the natural state model, the permeability and deep inflows are adjusted until the model matches the observed temperature distribution.

Many iterations of the natural state modelling process were required to obtain a satisfactory model of the pre-production state of Ohaaki. Since the last modeling work carried out in 2010 not much new temperature data has become available, but improvement of the temperature matches was achieved. Overall the 2010 model and the 2006 model were too hot at depth and this feature has been improved in the 2011 model.

5.5.1 Temperature Results

The natural state temperature profile obtained using the 2011 model for a typical East Bank well is shown in Figure 5. The field data is limited in this area but the model is matching the general profile well. The model temperatures show a similar profile for most blocks in this region.

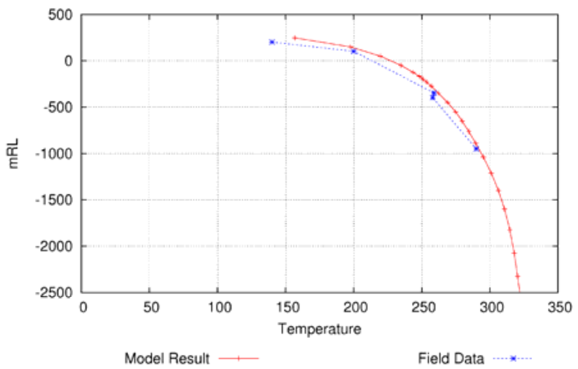

Figure 5. Temperature profile for a typical East Bank well.

The 2011 model shows a big improvement on the temperatures at depth; as many of the 2006 and 2010 model profiles had base temperatures nearing 350°C.

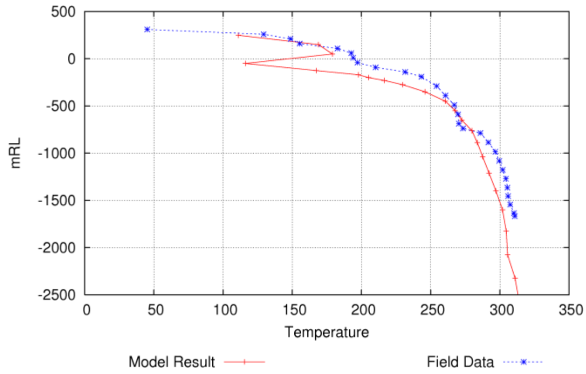

Figure 6. Temperature profile for a typical West Bank well.

As most of the wells on the West Bank are newer than on the East Bank, the temperature data for a typical West Bank well has been plotted at the corresponding time in the production history (**Error! Reference source not found.**). The model is showing a reasonable match to the field data for this well, except for the large temperature reversal at 0mRL.

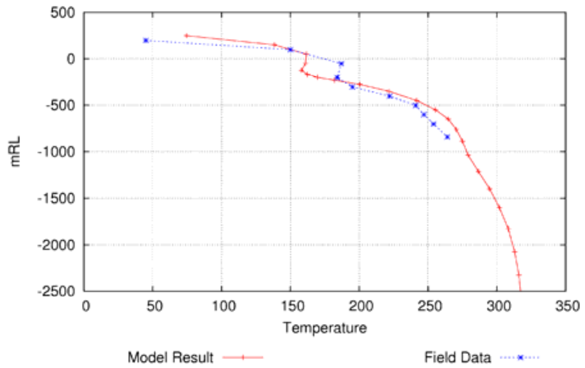

Figure 7. Temperature profile for a well at the margin of the reservoir and south of the East Bank.

Model results for a well at the margin of the reservoir are shown in Figure 7. The model shows a reasonable match, although from 0 to -250mRL the model is too cold and is too hot from -500mRL downwards. Calibration of this area of the model is ongoing.

5.6 Production History Modelling

Once the results from the natural state simulation have reached a satisfactory standard, the resulting pressures and temperatures for each block in the model grid are used as initial conditions for a production history simulation. For the simulation of the production history the feed zones of the wells were identified and then the production for each well was assigned to the corresponding block in the model. The period simulated is 1966 until the beginning of 2010.

5.6.1 Enthalpy Results

The match with field data for the enthalpies resulting from the model is quite varied. In some cases not enough boiling is shown in the model for a period of approximately 10 years from 1990-2000. A result for a well in the East Bank is shown in Figure 8. This well shows an initial increase of enthalpy at the start of production, followed by a slow decline. The model matches the general declining enthalpy trend very well but does not show the initial increase over the period 1990-1995, not enough boiling is occurring at this point in the model.

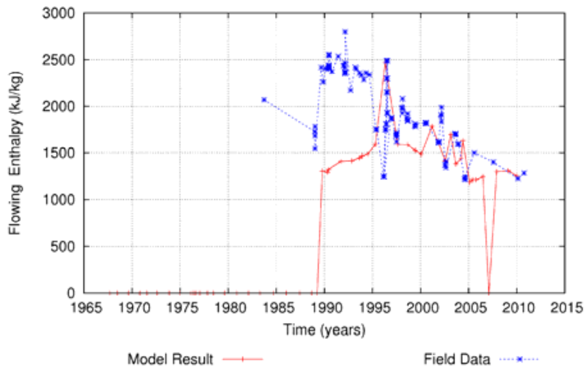

Figure 8. Enthalpy result for a typical East Bank well.

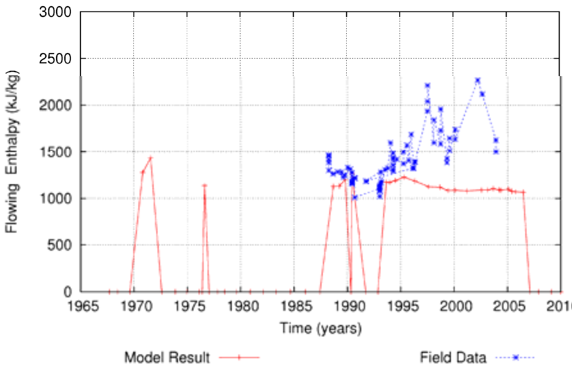

Figure 9. Enthalpy result for a typical West Bank well.

The enthalpy trend for a typical well on the West Bank seen in Figure 9 shows a different enthalpy trend – this well starts off at a low enthalpy which then increases over time. The model results do not follow this trend and not enough boiling is occurring from 1995 onwards, but the match for the previous times is reasonable. The total enthalpy match for all wells joined to separator 1 is shown in Figure 10, and the total match for separator 5 in **Error! Reference source not found.**. The enthalpy match for separator 1 is reasonable, showing the correct trend even if the model values are a little low.

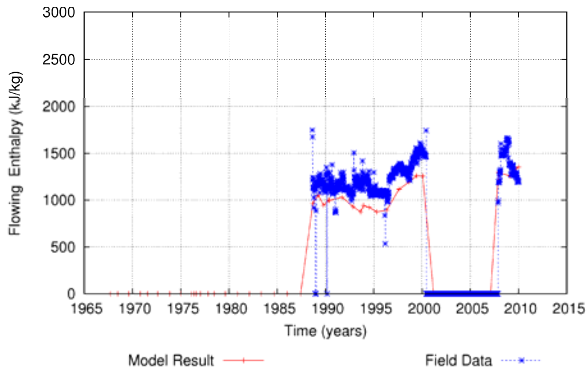

Figure 10. Enthalpy vs. Time for Separator 1.

When there are mis-matches in the history for individual wells that are large producers, this mismatch is also seen in the total enthalpy match. For example the mis-match seen over 1990 to 1995 in the East Bank well enthalpy (Figure 8) is echoed in the corresponding enthalpy history of separator 5 (Figure 11).

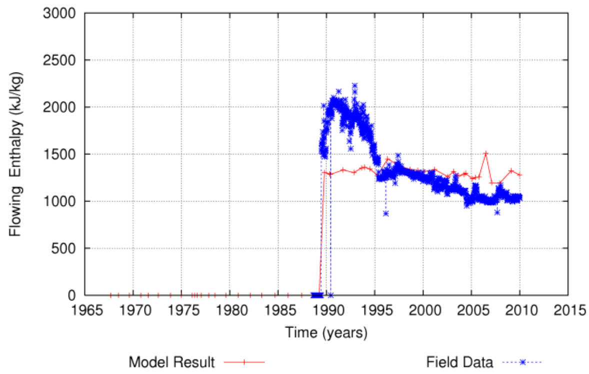

Figure 11. Enthalpy vs. Time for Separator 5.

Most enthalpy matches show a reasonable correlation to the field data; in areas where the enthalpy is too low in the model, the general trends are usually still matched. Also, most large mismatches occur in the earlier history and the latest enthalpy trends are generally more accurate. However, for some of the most recent wells, the model enthalpy is far too high and for others (a seen in Figure 9) the model enthalpy is far too low. More calibration work is required to improve some of the enthalpy matches.

5.6.2 Pressure History Results

The model pressures during the drawdown-recovery period are a good match for most wells. Some show a greater drawdown, and then greater recovery than the measured data, and this is often correlated with an enthalpy mismatch. Production pressures in the shallow East Bank reservoir are predicted well by the model. The result for a typical East Bank well is shown in Figure 12. The model is matching the drawdown from 1995 to 2000 very well. Production pressures in the deeper West Bank reservoir predicted by the model follow the same trend as the field data - Figure 13 shows the draw down history of a new deep West Bank well, which is matched accurately.

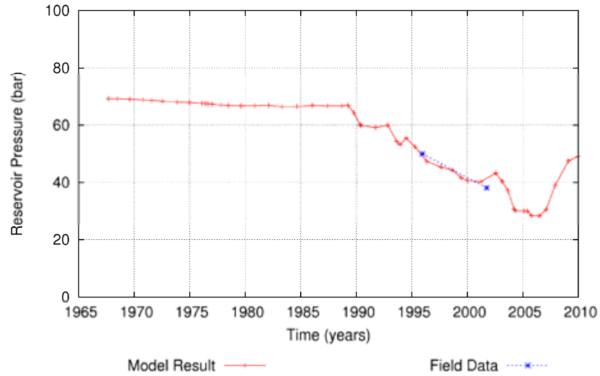

Figure 12. Pressure vs. Time for a typical shallow East Bank well.

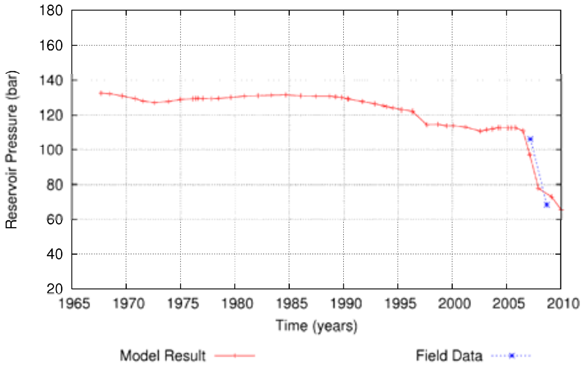

Figure 13. Pressure history for a typical deep West Bank well.

5.6.3 CO_2 Percent Mass Fraction Results

The CO_2 mass fraction data are difficult to match, and accurately predicting the movement of CO_2, gas and liquid, throughout the reservoir is a challenge.

CO_2 is poorly soluble in the liquid phase of water so most of it resides in the gas phase leading to a strong correlation between the overall CO_2 content and in-place gas saturation. At a constant pressure and temperature an increasing CO_2 content increases the gas saturation, reduces fluid mobility and causes the flowing enthalpy to be strongly dependent on the CO_2 content; the higher the CO_2 content, the higher the fluid enthalpy.

The changes in fluid enthalpy and CO_2 content over time are dependent on what is happening nearby in the reservoir, and what has happened previously within that area, and so there are many possible outcomes resulting from each small calibration change. Also, the in-place CO_2 mass fraction does not coincide with the flowing CO_2 mass fraction field data required to be matched - the flowing CO_2 mass fraction is much greater than the in place CO_2 mass fraction for gas saturations of 0.1 or higher

The flux of CO_2 into the base of the reservoir is altered through calibration. Changes in relative permeability can also alter the in–place CO_2 mass fraction. Permeability will not directly affect the CO_2 mass fraction, but initial gas saturation does, and so permeability and porosity changes can help with calibration of gas saturation. Figure 14 and Figure 15 show the CO_2 mass flow history for typical East and West Bank wells respectively. The results vary – the East bank has a good match, the West Bank shows a poor match.

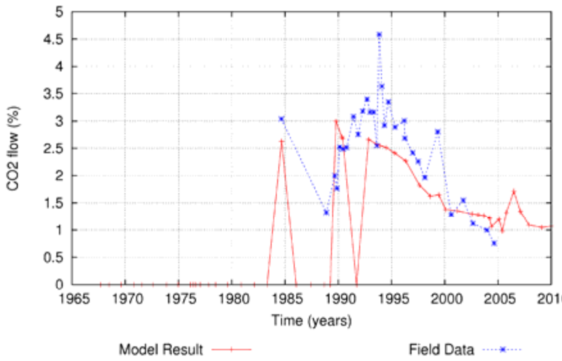

Figure 14. A typical history of CO_2 in the East Bank.

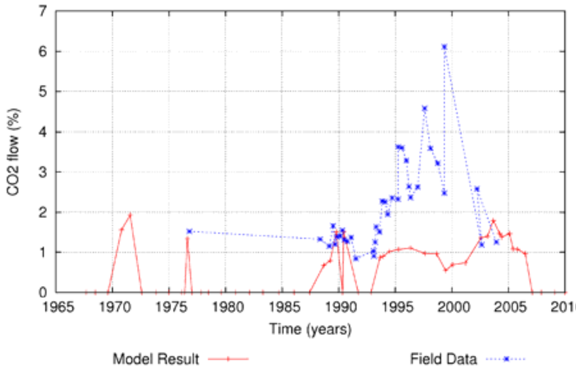

Figure 15. CO_2 fraction history for a typical West Bank well.

Calibration work on the CO_2 match is ongoing. Gaining a better grasp on the origin and location of CO_2 flows, as with other reservoir parameters, gives an overall better understanding of the behaviour of the Ohaaki system.

5.7 Modelling Difficulties

Aside from the field data extraction difficulty outlined in section 3 of this paper, another particular problem has been found when trying to calibrate the Ohaaki reservoir model. This difficulty appears to be particularly severe for models with a CO_2/water equation of state, but could be due to the interaction of any liquid and gas phases, as it has also been seen on layers near the unsaturated zone when using an air/water model.

In some cases a small change in the permeability structure resulted in a particular model block needing to change from a two phase state to compressed hot water. In the Ohaaki model the high CO_2 content can often make this phase change difficult and the natural state simulation takes a very large number of time steps to complete. Or, the time step may get so small that the simulation may never reach completion.

Unfortunately this problem makes it difficult to use the inverse modeling code iTOUGH2 [19] to assist with model calibration, and makes it hard to determine the sensitivities of the model to variation in parameter values.

6. FUTURE WORK

The 2011 model is providing a good representation of the Ohaaki geothermal system and is currently being used to simulate various development scenarios which will assist Contact Energy Limited with their field management and future planning.

As mentioned above some aspects of model calibration could be improved and this work is ongoing.

7. ACKNOWLEDGEMENTS

The authors wish to thank Contact Energy Ltd for permission to publish this paper.

8. REFERENCES

[1] S. Lee and L. Bacon, "Operational History of the Ohaaki Geothermal Field, New Zealand," in *World Geothermal Congress*, Kyushu-Tohoku, Japan, 2000, pp. 3211-3216.

[2] M. R. Blakely, M. J. O'Sullivan, and G. S. Bodvarsson, "A simple model of the Ohaaki Geothermal Reservoir," in *5th New Zealand Geothermal Workshop*, University of Auckland, 1983, pp. 11-16.

[3] J. A. Newson and M. J. O'Sullivan, "Modelling the Ohaaki Geothermal System," in *26th Workshop on Geothermal Reservoir Engineering*, Stanford University, Stanford, California, 2001, pp. 186-192.

[4] S. J. Zarrouk and M. J. O'Sullivan, "Recent Computer Modelling of the Ohaaki Geothermal System," in *(28th) New Zealand Geothermal Workshop*, University of Auckland, 2006.

[5] M. J. O'Sullivan and E. K. Clearwater, "Ohaaki Modelling Report," The University of Auckland (Uniservices), Auckland 2011 - BR1, March 2011 2011.

[6] R. G. Allis, "Heat Flow," in *Guide to Geophysics of the Volcanic and Geothermal Areas of the North Island, New Zealand.* vol. Miscellaneous Series 3, ed: The Royal Society of New Zealand, 1980, pp. 47-48.

[7] H. J.W., "The thermal and geochemical structure of the Broadlands -Ohaaki geothermal system, New Zealand.," *Geothermics,* vol. 19, pp. 151-185, 1990.

[8] R. B. Glover, T. M. Hunt, and C. M. Severne, "Impacts on development on a natural thermal feature and their mitigation - Ohaaki Pool, New Zealand," *Geothermics,* vol. 29, pp. 509-523, 2000.

[9] C. P. Wood, R. L. Brathwaite, and M. D. Rosenberg, "Basement structure, lithology and permeability at Kawerau and Ohaaki geothermal fields, New Zealand," *Geothermics,* vol. 30, pp. 461-481, 2001.

[10] A. J. Rae, M. D. Rosenberg, G. Bignall, G. N. Kilgour, and S. Milicich, "Geological results of production well drilling in the western steamfield, Ohaaki geothermal system:2005-2007," in *(29th) New Zealand Geothermal Workshop*, 2007.

[11] J. A. Newson, "Ohaaki Reservoir Workshop," Personal Communication ed. Taupo, 2011.

[12] A. Clotworthy, L. B., and B. Carey, "Operational History of the Ohaaki Geothermal Field, New Zealand.," in *World Geothermal Congress*, Florence, Italy, 1995, pp. 1797-1802.

[13] S. J. Zarrouk, M. J. O'Sullivan, and J. A. Newson, "Computer Modelling of the Ohaaki Geothermal System," in *(26th) New Zealand Geothermal Workshop*, University of Auckland, Auckland, 2004, pp. 114-120.

[14] T. M. Hunt, "Geophysical Exploration of the Broadlands (Ohaaki) Geotheraml Field: Review," in *(11th) New Zealand Geothermal Workshop*, University of Auckland, 1989, pp. 31-38.

[15] G. F. Risk, "Tests for resistivity boundary changes at Ohaaki New Zealand," in *(19th) Workshop on Geothermal Reservoir Engineering*, Stanford University, Stanford, California, 1994, pp. 117-123.

[16] S. Alcaraz, R. Lane, K. Spragg, S. Milicich, F. Sepulveda, and G. Bignall, "3D geological modelling using new Leapfrog Geothermal software," in *(36th) Workshop on Geothermal Reservoir Engineering*, Stanford University, Stanford, California, 2011.

[17] D. P. Bullivant, M. J. O'Sullivan, and G. A. Zyvoloski, "Enhancements of the Mulkom Geothermal Simulator," in *(13th) New Zealand Geothermal Workshop*, University of Auckland, 1991, pp. 175-182.

[18] K. Pruess, "TOUGH2, a general-purpose numerical simulator for multiphase fluid and heat flow," Lawrence Berkeley Laboratory, Berkeley, California1991.

[19] S. Finsterle, *ITOUGH2 User's Guide Version 2.2*: Lawrence Berkeley Laboratory, University of California, 1993.